

Molecular Thermodynamics Approach on Phase Equilibria of Dendritic Polymer Systems

Jeong Gyu Jang, Ho Bum Park and Young Moo Lee[†]

National Research Laboratory for Membrane, School of Chemical Engineering,
College of Engineering, Hanyang University, Seoul 133-791, Korea
(Received 15 October 2002 • accepted 2 December 2002)

Abstract—We suggest a molecular thermodynamic framework to describe the phase behavior of dendritic polymer systems. The proposed model, which is based on the lattice cluster theory, contains correlations of molecular structure and specific interactions such as hydrogen bonding to the phase equilibria of branch-structured polymer systems. We examine liquid-liquid equilibria (LLE) of hyperbranched polymer solutions and vapor-liquid equilibria (VLE) of dendrimer solutions in the viewpoints of effects of a branched structure and specific interaction formations among endgroups of dendritic polymer and solvent molecules. We investigate VLE of dendrimer/solvent (Benzyl Ether Dendrimer/Toluene) systems by the combination of a new lattice-based model and atomistic simulation technique. The interaction energy parameters are obtained by the pairs method [Baschnagel et al., 1991] including Monte Carlo simulation with excluded volume constraint. In the pairs method [Baschnagel et al., 1991], we do not simulate the whole molecule as in molecular dynamics or molecular mechanics, but only monomer segments interacting with solvent molecules. The proposed model shows improvements in prediction for both phase equilibria (VLE and LLE) due to the branched structure and specific interaction due to endgroups at periphery of dendritic polymer molecule. Atomic simulation technique gives good result in prediction without fitting variables. Our results show that the specific interactions between the endgroup and the solvent molecule play an important role in phase behavior of the given systems.

Key words: Dendritic Polymer, Molecular Thermodynamics, Molecular Simulation, LLE, VLE, Structure, Specific Interaction

INTRODUCTION

Macromolecular architecture is receiving increasing interest as the search for new tailor-made polymeric materials with strictly specified properties intensifies. Many research groups are now focusing their interest on dendritic macromolecules (dendrimer and hyperbranched polymers).

These consist of a central core, concentrated “shells” and an external surface. Each family of dendrimers, i.e., dendrimers made with the same repeat unit, consists of different generations, each corresponding to a different number of shells around the core. The architecture induces new and intriguing properties for the polymers, such as low viscosity, miscibility, high reactivity and high solubility in various solvents [Johansson et al., 1996]. The high degree of branching for dendritic polymers has some consequences, e.g., no crystallization and no inter-chain entanglement have been observed [Fréchet, 1994]. This gives rise to poor mechanical properties but good solubility and decreased melt viscosity [Hawker et al., 1995]. For dendrimers, the variety of molecular structure, size, shape, topology, flexibility and surface chemistry offer many possible applications for new materials. These include nanoscale catalysts and reaction vessels, micelle mimics, magnetic resonance agents, immuno-diagnostics, agents for delivering drugs into cells, chemical sensors, information-processing materials, high-performance polymers, adhesives and coatings, separation media, and molecular an-

tennae for absorbing light energy and funneling it to a central core [Dagani, 1996]. Most of the ideas focus on the peculiarities of the dendritic interior and a large number of endgroups for their rationalization. Despite the wealth of possible application, little work has been reported on the thermodynamic properties of solution containing dendritic polymers.

In this work, we propose a lattice-based thermodynamic framework and present the molecular thermodynamic approach for the phase behavior of dendritic polymer systems using molecular simulation. The framework includes thermodynamic modeling on the branched structure and interactions due to endgroups at the periphery of dendritic polymers, both of which are major factors for characteristics of dendritic polymer systems. Although molecular thermodynamic framework for polymer systems is well established in calculation for their thermodynamic properties dealing with new polymer systems, mathematical models still require tedious experimental work to determine their interaction parameters. There are many difficulties in actual application due to the absence of detailed information regarding each component. In the case of dendrimer, a difficult synthesis using multiple repetitive procedures is also a severe obstacle to industrial application. Thus, molecular simulation will be a useful and desirable tool to determine interaction parameters without experimental efforts.

The standard lattice model of polymers was solved in the simple mean field approximation independently by Flory [1953] and Huggins [1941], and the treatment of the former is customarily termed Flory-Huggins theory. Lattice theories have contributed much to the understanding of polymer solutions. In addition, much work has been done to improve the mathematical solution of the lattice model including chain connectivity and non-random mixing [Gug-

[†]To whom correspondence should be addressed.

E-mail: ymlee@hanyang.ac.kr

[‡]This paper is dedicated to Professor Baik-Hyon Ha on the occasion of his retirement from Hanyang University.

genheim, 1952; Aranovich and Donhue, 1996; Kim et al., 2001]. However, the mean field approximation has been found to be quantitatively deficient in some aspects.

The lattice models are supplemented by an entropic contribution to interaction energies. Barker and Fock [1953] developed a quasi-chemical method to account for the specific interaction. ten Brinke and Karasz [1984] have developed an incompressible model of binary mixture with the specific interaction. Using a quasi-chemical approach to treat the nonrandom character of the polymer solution, Panayiotou and Vera [1980] and Renuncio and Prausnitz [1976] have developed an improved FOVE equation of state model, and Panayiotou [1987], and Sanchez and Balazs [1989] have generalized the lattice fluid model to account for the specific interaction. In 1990, Veystman [1990] proposed an expression for the hydrogen bonds contribution to the free energy of fluid, valid for the general case. Veystmans approach is widely used in thermodynamic modeling of systems associated with hydrogen bonding because of generality and simplicity [Jung et al., 2002]. Furthermore, Freed et al. [Freed, 1985; Bawendi et al., 1988a, b] reported a complicated lattice field theory for polymer solutions, which is formally an exact mathematical solution of the Flory-Huggins lattice. Most of these lattice theories, however, fail to yield a dependence of solution properties on the polymer architecture. In 1987, Nemirovsky et al. [1987] proposed a new model with the effect of branched architecture of polymer structure being considered. They have given a systematic expansion of the partition function of polymer using the well-known lattice cluster theory (LCT) [Freed and Bawendi, 1989; Dudowicz et al., 1991; Freed and Dudowicz, 1992; Dudowicz and Freed, 1991; Nemirovsky et al., 1992].

Molecular simulation methods such as molecular mechanics, molecular dynamics and Monte Carlo simulation are applied to several polymer systems [Allen and Tildesley, 1987; Monnerie and Suter, 1994; Burtkert and Allinger, 1982; Roe, 1991]. However, such full atomistic molecular simulations have a severe limitation in calculation power and in time scale [Jo and Choi, 1997].

The coarse-grained model [Binder and Heermann, 1988] is proposed as an alternative for this problem. It is successful in predicting physical properties of polymeric materials less sensitive to the exact chemical structure but does not include detailed information on the structure of materials. Some efforts are made to improve the correlation of structure in the coarse-grained model by introducing additional molecular parameters [Baschnagel et al., 1991] and imposing several potential functions [Kim et al., 1994]. The polymer reference interaction site model theory [Schweizer and Curro, 1989] is employed to study phase behaviors of polymer systems. In 1992, Fan et al. [1992] proposed a new approach to predict phase diagrams by combining Flory-Huggins theory and Monte Carlo simulation method. Jo and Choi [1997] combined an equation of state theory and molecular simulation on the basis of the coarse-grained model to analyze the surface phenomena of polymeric materials. Chang et al. examined the validity and accuracy of approximation in equation of state model by comparison between theoretical prediction and simulation results [Chang and Kim, 1998].

In this study, we propose a lattice model based on the lattice cluster theory (LCT), which includes highly branched structure effect and interaction factors due to numerous endgroups in the periphery of the molecules. We compare the proposed model with experimen-

tal data on phase equilibria of dendritic polymer systems including hyperbranched polymer aqueous system and organic dendrimer solutions. Using an atomistic Monte Carlo approach, we investigate the application of simulation technique to phase behavior predictions for dendritic polymer systems.

MODEL DEVELOPMENT

We use a similar approach to the model developed by Panayiotou and Sanchez [1991] to introduce the contribution of specific interactions between molecules. We consider a system of N_s molecules of solvents, N_p molecules of polymers. In the general case, there are m types of specific donor groups and n types of specific interaction acceptor groups distributed in the molecules of the system. Let i kind molecules have d_i , the number of donor groups, and a_i , the number of acceptor groups. We assume that all donor sites are only one type of donating and acceptor sites are only one type of accepting. In order to get the free energy of mixing for a polymer solution system, we assume that the number of configurations also factors into two independent parts. We consider only the physical intermolecular interaction in one factor, while the specific interaction in the other. This means that the intermolecular forces are divided into physical and chemical forces. Then, the number of configurations can be expressed as follows:

$$\Omega = \Omega_{LCT} \Omega_s \quad (1)$$

Helmholtz free energy of mixing can be added as follows:

$$\Delta A = \Delta A^{LCT} + \Delta A^s \quad (2)$$

where ΔA^{LCT} and ΔA^s are physical and chemical contributions to the Helmholtz free energy, respectively. We develop a model on the basis of "the coupling" approximation of interaction [Panayiotou and Sanchez, 1991]. In this assumption, we take into account the one bond contribution to Helmholtz energy for specific interaction contribution, while LCT considers multi-bond contribution to physical force by cluster expansion. Thus, we consider specific interaction only between adjacent specific interaction donor and specific interaction acceptor.

We first place the polymer solution on a lattice with N total sites. Each monomer or a solvent molecule occupies one lattice site and each polymer molecule is assumed to occupy M lattice sites. The lattice is assumed to be fully occupied. Volume fractions of polymer (ϕ_2) and solvent (ϕ_1) in solution are

$$\phi_1 = N_s/N \quad (3)$$

$$\phi_2 = N_p M/N \quad (4)$$

Each site has z nearest neighboring sites. Physical attractive interaction in this system are characterized by a parameter ϵ ,

$$\epsilon = \epsilon_{11} + \epsilon_{22} - 2\epsilon_{12} \quad (5)$$

where ϵ_{11} is the energy of a solvent-solvent contact, ϵ_{22} is the energy of a non-bonded polymer segment-segment contact, and ϵ_{12} is the energy of a polymer segment-solvent contact. Subscript 1 refers to 1-component (solvent) and subscript 2 refers to 2-component (polymer).

1. Lattice Cluster Theory

Freed et al. [Nemirovsky et al., 1987; Freed and Bawendi, 1989;

Dudowicz et al., 1991; Freed and Dudowicz, 1992; Dudowicz and Freed, 1991; Nemirovsky et al., 1992] have proposed the LCT applicable to arbitrary chain architecture. It gives general calculation for an incompressible blend of two different polymers of arbitrary architectures. The polymer-solvent system is but a special limit of a blend in which one of the chains is quite short. A given chain architecture may be represented by a linear sequence or complicated branching pattern in which monomers have specified structure. However, all chains of given architecture are considered to have the same bonding topology and not to have small closed loops. Nemirovsky et al. [1987] described how the theory could be derived and Dudowicz et al. [1991] generalized the theory to branched polymer architectures, composed of structured monomer. In this study, Helmholtz free energy of the system is expanded in a double power series of $1/z$ and $\epsilon/k_B T$, where k_B is the Boltzmann constant and T is the absolute temperature in Kelvin. We truncate the series at the second order in $1/z$ and the fourth order in $\epsilon/k_B T$. The free energy of mixing for the polymer-solvent binary mixture is given by [Freed and Dudowicz, 1992; Nemirovsky et al., 1992]

$$\Delta A = \Delta A^{LCT} + \Delta A^S = \Delta A^{ath} + \Delta A^{int} + \Delta A^S \quad (6)$$

where ΔA^{int} , ΔA^{ath} and ΔA^S are the contribution of the attractive interaction, the athermal limit of the entropy of mixing and the specific interaction formation, respectively.

$$\frac{\beta \Delta A^{ath}}{N} = \frac{\phi_2}{M} \ln \phi_2 + (1 - \phi_2) \ln(1 - \phi_2) + a^{(0)} \phi_2 (1 - \phi_2) + a^{(1)} \phi_2^2 (1 - \phi_2) + a^{(2)} \phi_2^3 (1 - \phi_2) \quad (7)$$

where $a^{(i)}$ are parameters that depend only on the architecture of the polymer molecules

$$\begin{aligned} \beta \Delta A^{int}/N = & A^{(1)} \phi_2 (1 - \phi_2) + (A^{(2)} + B^{(3)}) \phi_2^2 (1 - \phi_2)^2 + A^{(3)} \phi_2^2 (1 - \phi_2)^2 (1 - 2\phi_2)^2 \\ & + A^{(4)} \phi_2^2 (1 - \phi_2)^2 [1 - 6\phi_2 (1 - \phi_2) (3\phi_2^2 - 3\phi_2 + 2)] \\ & + (B^{(1)} + B^{(2)}) \phi_2 (1 - \phi_2)^2 + B^{(4)} \phi_2^3 (1 - \phi_2)^2 \\ & + C^{(1)} \phi_2 (1 - \phi_2)^2 (1 - 2\phi_2)^2 + C^{(2)} \phi_2 (1 - \phi_2)^3 \\ & + C^{(3)} \phi_2^2 (1 - \phi_2)^3 (1 - 3\phi_2) + C^{(4)} \phi_2 (1 - \phi_2)^4 \end{aligned} \quad (8)$$

$A^{(i)}$, $B^{(i)}$ and $C^{(i)}$ are parameters associated with the architecture of the polymer, for attractive interaction and the coordination number. These parameters are listed in Table 2. The combinatorial numbers, $N_{(\alpha)}$ and $N_{(\alpha, \beta)}$, describe the architecture of polymers. The definitions [Freed and Dudowicz, 1992] of the structure parameters are given as follows: M is the number of segments in each polymer molecule; $N_{(1)}$ is the number of bonds in each polymer molecule; $N_{(2)}$ is the number of ways in which three bonds intersect; $N_{(3)}$ is the number of ways in which three consecutive bonds can be chosen; $N_{(\perp)}$ is the number of ways in which three bonds meet at a lattice site for a polymer chain; $N_{(1,1)}$ is the number of distinct ways of selecting two non-sequential bonds on the same chain; and $N_{(1,2)}$ is the number of distinct ways of selecting one bond and two sequential bonds on the same chain.

In the LCT model, dendritic polymer structure is characterized by three parameters, the generation number (g), the separator length (n) that is the number of bonds between branch points and the core segment (n_0) between zeroth generation points. The combinatorial numbers, $N_{(\alpha)}$ and $N_{(\alpha, \beta)}$, are calculated by counting indices for these types of polymers. Geometric parameters for dendritic polymer are listed in Table 1.

Table 1. Geometric parameters for dendritic polymers

	General structure	Structure with $n=1$
M	$4(2^{g-1}-1)n + 2^g \times n_1 + n_0 + 2$	$4(2^{g-1}-1)n + n_0 + 2$
N_1	$M-1$	
N_2	$4(2^{g-1}-1)(n-1) + 2^g \times n_1 + 3N_{\perp} + n_0$	$4(2^{g-1}-1)(n-1) + 3N_{\perp} + n_0$
N_3	$4(2^{g-1}-1)(n-2) + 6N_{\perp} + n_0 - 1 + 2^g \times n_1$	$4(2^{g-1}-1) \times 2 + n_0 - 3$
N_{\perp}	$2(2^{g-1}-1)$	
$N_{1,1}$	$N_1 C_2 - N_2$	
$N_{1,2}$	$N_2 \times (N_1 - 2) - N_3 - 3N_{\perp}$	

Table 2. Parameters for lattice cluster theory

$A^{(1)}$	$(\beta \epsilon) z / 2$
$A^{(2)}$	$-(\beta \epsilon)^2 z / 4$
$A^{(3)}$	$-(\beta \epsilon)^3 z / 12$
$A^{(4)}$	$-(\beta \epsilon)^4 z / 48$
$B^{(1)}$	$-\beta \epsilon N(1)$
$B^{(2)}$	$(\beta \epsilon / z)(2N(2) + N(3) + 3N(\perp) + N(1, 2) - N(1)N(2)M)$
$B^{(3)}$	$-(2\beta \epsilon / z)N(1)(2N(1) + N(1, 1) - [N(1)]^2 M)$
$B^{(4)}$	$-(4\beta \epsilon / z)[N(1)]^3$
$C^{(1)}$	$-((\beta \epsilon)^2 / 2)N(1)$
$C^{(2)}$	$-(\beta \epsilon)^2 N(2)$
$C^{(3)}$	$-(\beta \epsilon)^2 [N(1)]^2$
$C^{(4)}$	$-((\beta \epsilon)^2 / 2)(N(1, 1) - [N(1)]^2 M)$
$a^{(0)}$	$(1/z)[N(1)]^2 + (1/z^2)\{-4N(1)N(2) + (8/3)[N(1)]^3 - 2N(1)N(3) + [N(2)]^2 - 2N(1)N(1, 2) - N(1)N(2)M + 2[N(1)]^4 + 2[N(1)]^2 N(1, 1) - [N(1)]^2 M\} - 6N(1)N(\perp)$
$a^{(1)}$	$(1/z^2)\{(8/3)[N(1)]^3 + 2[N(1)]^4 + 2[N(1)]^2 N(1, 1) - [N(1)]^2 M\}$
$a^{(2)}$	$(1/z^2)2[N(1)]^4$

where $N(\alpha) = N_{\alpha}/M$ ($\alpha = 1, 2, 3$ or \perp) and $N(\alpha\beta) = N_{\alpha, \beta}/M$ ($\alpha = 1$ or 2)

2. Specific Interaction Contribution to the Free Energy

In this work, we use the “donor-acceptor” hydrogen bonding concept in order to take into account the specific interactions and assume that the specific interaction formation is a kind of bonding. We consider a system containing molecules of k species, and N_i is the number of i th kind molecules. Any molecule of the i th kind has d_i donor sites and a_i acceptor sites. For simplicity, we assume that all donor sites are only one type of donating and acceptor sites are only one type of accepting. We assume that association bonds are formed as a specific interaction occurs. A donor site of an i th kind molecule can form a specific interaction with an acceptor site of a j th kind molecule if the sites are located in the adjacent cells. Such a bond is referred to as (i, j) bond and the free energy of an (i, j) bond formation is F_{ij}^S . There are entropic contributions associated with the specific interactions. From the number of ways, Ω_S , of distributing M_{ij} bonds among the functional groups of the system, we obtain the additional contribution to Helmholtz energy as follows [Veystman, 1990; Panayiotou and Sanchez, 1991; Jang and Bae, 2001]:

$$\begin{aligned} A^S = & \sum_{i=1}^k \sum_{j=1}^k M_{ij} F_{ij}^S + k_B T \sum_{i=1}^k \sum_{j=1}^k M_{ij} \ln \left(\frac{e N M_{ij}}{N_i d_i - \sum_{m=1}^k M_{im} \left(N_j a_j - \sum_{n=1}^k M_{jn} \right)} \right) \\ & + k_B T \sum_{i=1}^k N_i d_i \ln \left(1 - \sum_{j=1}^k \frac{M_{ij}}{N_i d_i} \right) + k_B T \sum_{j=1}^k N_j a_j \ln \left(1 - \sum_{i=1}^k \frac{M_{ij}}{N_j a_j} \right) \end{aligned} \quad (9)$$

where, M_{ij} is the number of (i, j) pair specific interaction formation. We use a mean-field approximation in calculating the probability that a specific acceptor j will be proximate to a given donor i [Panayiotou and Sanchez, 1991]. In equilibrium, the free energy A^S at a given M_{ij} is obtained by minimizing with respect to M_{ij}

$$\left(\frac{\partial A^S}{\partial M_{ij}}\right)_{T, N_i, M_{rs}} = 0 \quad (10)$$

$$A^S = k_B T \sum_{i=1}^k \sum_{j=1}^k M_{ij} + k_B T \sum_{i=1}^k N_i d_i \ln \left(1 - \frac{\sum_{j=1}^k M_{ij}}{N_i d_i}\right) + k_B T \sum_{j=1}^k N_j a_j \ln \left(1 - \frac{\sum_{i=1}^k M_{ij}}{N_j a_j}\right) \quad (11)$$

where M_{ij} are determined by the set of quadratic equations from the relation of minimizing conditions

$$N M_{ij} = \left(N_i d_i - \sum_{m=1}^k M_{im}\right) \left(N_j a_j - \sum_{n=1}^k M_{nj}\right) \exp\left(-\frac{F_{ij}^S}{k_B T}\right) \quad (12)$$

Eqs. (11) and (12) give the excess free energy due to specific interaction formation.

3. Correlating Equations

The equation for the chemical potentials of solvent is obtained as follows:

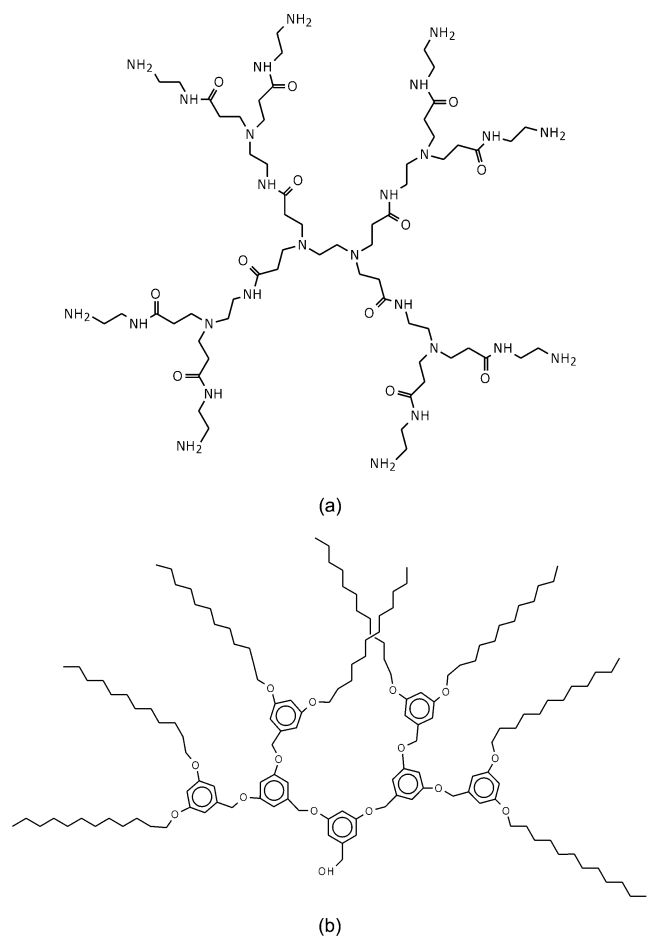


Fig. 1. (a) Polyamidoamine dendrimer generation 3. (b) Benzyl dodecyl dendrimer generation 3.

$$\mu_k = \left(\frac{\partial A}{\partial N_k}\right)_{T, N_j} = \left(\frac{\partial A}{\partial N_k}\right)_{T, N_j, \{M_{ij}\}} + \sum_i^m \sum_j^n \left(\frac{\partial A}{\partial M_{ij}}\right)_{T, \{N_j\}, \{M_{rs}\}} \left(\frac{\partial M_{ij}}{\partial N_k}\right)_{T, N_j} \quad (13)$$

But from Eq. (10) it simplifies to

$$\mu_k = \mu_k^{LCT} + \mu_k^S = \left(\frac{\partial A^{LCT}}{\partial N_k}\right)_{T, N_j, \{M_{ij}\}} + \left(\frac{\partial A^S}{\partial N_k}\right)_{T, N_j, \{M_{ij}\}} \quad (14)$$

Therefore, the chemical potential for physical contribution is given as the following equation:

$$\mu_1 = \mu_1^{LCT} + \mu_1^H \quad (15)$$

$$\mu_1^{LCT} = \frac{A^{LCT}}{N} - \phi_2 \frac{\partial(A^{LCT}/N)}{\partial \phi_2} \quad (16)$$

$$\begin{aligned} \beta \mu_1^{LCT} = & \ln(1 - \phi_2) + \left(1 - \frac{1}{M}\right) \phi_2 + a^{(0)} \phi_2^2 - a^{(1)} \phi_2^2 (1 - 2\phi_2) - a^{(2)} \phi_2^3 (2 - 3\phi_2) \\ & + A^{(1)} \phi_2^2 - (A^{(2)} + B^{(3)}) \phi_2^2 (1 - \phi_2) (1 - 3\phi_2) \\ & - A^{(3)} \phi_2^2 (1 - \phi_2) (1 - 2\phi_2) (1 - 9\phi_2 + 10\phi_2^2) \\ & - A^{(4)} \phi_2^2 (1 - \phi_2) (1 - 27\phi_2 + 138\phi_2^2 - 294\phi_2^3 + 306\phi_2^4 - 126\phi_2^5) \\ & + (B^{(1)} + B^{(2)}) 2\phi_2^2 (1 - \phi_2) - B^{(4)} 2\phi_2^2 (1 - \phi_2) (1 - 2\phi_2) \\ & + C^{(1)} 2\phi_2^2 (1 - \phi_2) (1 - 2\phi_2) (3 - 4\phi_2) + C^{(2)} 3\phi_2^2 (1 - \phi_2)^2 \\ & - C^{(3)} \phi_2^2 (1 - \phi_2)^2 (1 - 10\phi_2 + 15\phi_2^2) + C^{(4)} 4\phi_2^2 (1 - \phi_2)^3 \end{aligned} \quad (17)$$

Structures of target molecules are given in Fig. 1. We simplify these

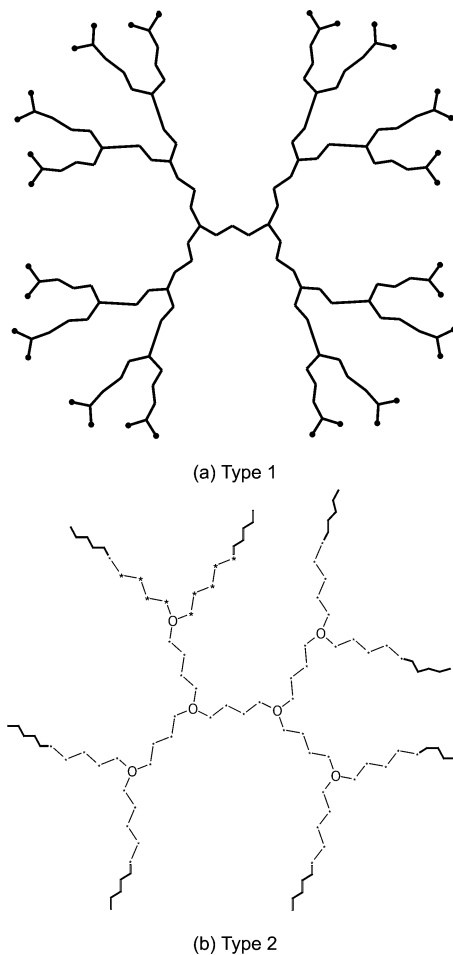


Fig. 2. (a) Simplified structure of polyamidoamine dendrimer generation 3. (b) Simplified structure of benzyl dodecyl dendrimer generation 3.

structures as two types in Fig. 2. Given dendrimers are characterized by three or four parameters. Indices are calculated for the given structure, so that those cannot represent a general case of dendrimer. Those values are listed in Table 1.

We assume that solvent molecule has one donor site and one acceptor site. The dendrimer molecules have acceptor sites only: $d_1=1$, $a_1=1$. The d_2 has the same value as the number of endgroups of polymer molecule. There is a possibility that the inner group of dendrimer forms a specific interaction with solvent. Here, we assume that those possibilities are low. Then, there are two types of specific interactions in the given systems. Helmholtz free energy and chemical potential of solvent are given as

$$\beta A^S = M_{11} + M_{12} + N_1 d_1 \ln \left(1 - \frac{M_{11} + M_{12}}{N_1 d_1} \right) + N_1 a_1 \ln \left(1 - \frac{M_{11}}{N_1 a_1} \right) + N_2 a_2 \ln \left(1 - \frac{M_{12}}{N_2 a_2} \right) \quad (18)$$

$$\mu_i^S = -\partial A^S / \partial N_i \quad (19)$$

$$\beta \frac{\partial A^S}{\partial N_1} = \beta \mu_1^S = d_1 \ln \left(1 - \frac{M_{11} + M_{12}}{N_1 d_1} \right) + \frac{d_1 (M_{11} + M_{12})}{N_1 d_1 - M_{11} + M_{12}} + a_1 \ln \left(1 - \frac{M_{11}}{N_1 a_1} \right) + \frac{a_1 M_{11}}{N_1 a_1 - M_{11}} = d_1 \ln \left(1 - \frac{v_{11} + v_{12}}{\phi_1 d_1} \right) + \frac{d_1 (v_{11} + v_{12})}{\phi_1 - v_{11} - v_{12}} + a_1 \ln \left(1 - \frac{v_{11}}{\phi_1 a_1} \right) + \frac{a_1 v_{11}}{\phi_1 a_1 - v_{11}} \quad (20)$$

where $v_{11} = M_{11}/N_1$, and $v_{12} = M_{12}/N_2$

The minimizing conditions of Eq. (10) give

$$NM_{11} = (N_1 d_1 - M_{11} - M_{12})(N_1 a_1 - M_{11}) \exp \left(-\frac{F_{11}^S}{k_B T} \right) \quad (21)$$

$$NM_{12} = (N_1 d_1 - M_{11} - M_{12})(N_2 a_2 - M_{12}) \exp \left(-\frac{F_{12}^S}{k_B T} \right) \quad (22)$$

Eqs. (21) and (22) are equivalent to

$$v_{11} = (\phi_1 d_1 - v_{11} - v_{12})(\phi_1 a_1 - v_{11}) \exp \left(-\frac{F_{11}^S}{k_B T} \right) \quad (23)$$

$$v_{12} = (\phi_1 d_1 - v_{11} - v_{12}) \left(\frac{\phi_2}{M} a_2 - v_{12} \right) \exp \left(-\frac{F_{12}^S}{k_B T} \right) \quad (24)$$

By rearranging Eqs. (23) and (24), we have

$$v_{11} = \frac{(a_1 + d_1) \phi_1 - v_{12} + 1/A_{11}}{2} - \frac{\sqrt{[(a_1 + d_1) \phi_1 - v_{12} + 1/A_{11}]^2 - 4a_1 \phi_1 (d_1 \phi_1 - v_{12})}}{2} \quad (25)$$

$$v_{12} = \frac{d_1 \phi_1 + a_2 \phi_2 / M - v_{11} + 1/A_{12}}{2} - \frac{\sqrt{(d_1 \phi_1 + a_2 \phi_2 / M - v_{11} + 1/A_{12})^2 - 4a_2 \phi_2 (d_1 \phi_1 - v_{11}) / M}}{2} \quad (26)$$

where $A_{11} = \exp(-F_{11}^S/k_B T)$, and $A_{12} = \exp(-F_{12}^S/k_B T)$

The activity of solvent a_1 is then

$$\ln a_1 = \beta \Delta \mu_1 = \beta \Delta \mu_1^{CT} + \beta \Delta \mu_1^S = \ln(1 - \phi_2) + \left(1 - \frac{1}{M} \right) \phi_2 + a^{(0)} \phi_2^2 - a^{(1)} \phi_2^2 (1 - 2\phi_2) - a^{(2)} \phi_2^3 (2 - 3\phi_2) + A^{(1)} \phi_2^2 - (A^{(2)} + B^{(3)}) \phi_2^2 (1 - \phi_2) (1 - 3\phi_2) - A^{(3)} \phi_2^2 (1 - \phi_2) (1 - 2\phi_2) (1 - 9\phi_2 + 10\phi_2^2)$$

$$-A^{(4)} \phi_2^2 (1 - \phi_2) (1 - 27\phi_2 + 138\phi_2^2 - 294\phi_2^3 + 306\phi_2^4 - 126\phi_2^5) + (B^{(1)} + B^{(2)}) 2\phi_2^2 (1 - \phi_2) - B^{(4)} 2\phi_2^3 (1 - \phi_2) (1 - 2\phi_2) + C^{(1)} 2\phi_2^2 (1 - \phi_2) (1 - 2\phi_2) (3 - 4\phi_2) + C^{(2)} 3\phi_2^2 (1 - \phi_2)^2 - C^{(3)} \phi_2^2 (1 - \phi_2)^2 (1 - 10\phi_2 + 15\phi_2^2) + C^{(4)} 4\phi_2^2 (1 - \phi_2)^3 + d_1 \ln \left(1 - \frac{v_{11} + v_{12}}{\phi_1 d_1} \right) + \frac{d_1 (v_{11} + v_{12})}{\phi_1 - v_{11} - v_{12}} + a_1 \ln \left(1 - \frac{v_{11}}{\phi_1 a_1} \right) + \frac{a_1 v_{11}}{\phi_1 a_1 - v_{11}} \quad (27)$$

Since the pure solvent has been chosen as the standard state, $a_1 = P/P_1^0$, to the approximation that the vapor is an ideal gas. P is the system pressure and P_1^0 is the vapor pressure of pure solvent at the system temperature.

4. Simulation Technique

BlendsTM, a component of the commercial software *Cerius²* from Molecular Simulation Inc, is used for simulation. This approach generates energetically favorable configurations by employing a Monte Carlo technique that includes excluded-volume constraints. The excluded-volume constraint method is applied in a variety of situations to sample energetics of molecules in simple or complex topological environments [Panayiotou and Sanchez, 1991]. The excluded-volume constraint method is a modified version of Blanco's molecular silverware algorithm. It aligns the molecules so that their van der Waals surfaces are barely touching. The details of the procedure used in this study are given elsewhere [Fan et al., 1992]. The segmental units of dendrimer molecule and solvent molecule are modeled and minimized energetically on the basis of the force field DREIDING 2.21. A generic force field, DREIDING, is useful for predicting structures and dynamics of organic, biological, and main-group inorganic molecules [Blanco, 1991]. Covalent interactions may be described by terms such as bond, valence angle, torsion, and hybridization terms; terms describing nonbonded interactions including van der Waals, electrostatic and hydrogen-bonding interactions. From this method, four Boltzmann-averaged pairwise interaction energy values (ϵ_{11} , ϵ_{12} , ϵ_{21} , and ϵ_{22}) for each model segment are obtained. Temperature effects are taken into account by weighting the distribution by the Boltzmann factor, $\exp(-\epsilon_{ij}/k_B T)$. The pairs method consists of several steps to apply the excluded volume constraint method. We make a brief description of the procedure. First, we construct the monomer repeat unit of dendritic polymer and solvent molecule. The structures are optimized by using energy minimization. Molecule 1 and molecule 2 (monomer repeat unit or solvent molecule) are located at the geometric center. Then, in order to specify the orientation of molecule 2 with respect to molecule 1, the Euler angles (α , β , γ) are chosen randomly. Molecule 2 is translated along the vector randomly chosen until the van der Waals surfaces of each molecule just touch each other. After the translation, the pair interaction energy of this specific configuration is calculated. These steps are repeated and ϵ_{ij} is calculated by averaging the entire accepted configurations. *Blends* in *Cerius* gives three types of interaction energies: van der Waals interaction, coulombic interaction and hydrogen bond interaction. Target materials for simulation have no hydrogen bonding formation site. Therefore, we calculate the total interaction energies with van der Waals and coulombic interactions.

RESULTS AND DISCUSSION

We first examine phase behaviors of hyperbranched polymer/

Table 3. The structures of the polymers

	Structure
Generation 2	$[O[CH_2C(CH_2H_5)(CH_2O^-)_2]_2A_4B_8$
Generation 3	$[O[CH_2C(CH_2H_5)(CH_2O^-)_2]_2A_4A_8B_{16}$
Generation 4	$[O[CH_2C(CH_2H_5)(CH_2O^-)_2]_2A_4A_8A_{16}B_{32}$

A=[COC(CH₃)(CH₂O⁻)₂]; B=[COC(CH₃)(CH₂OH)₂]

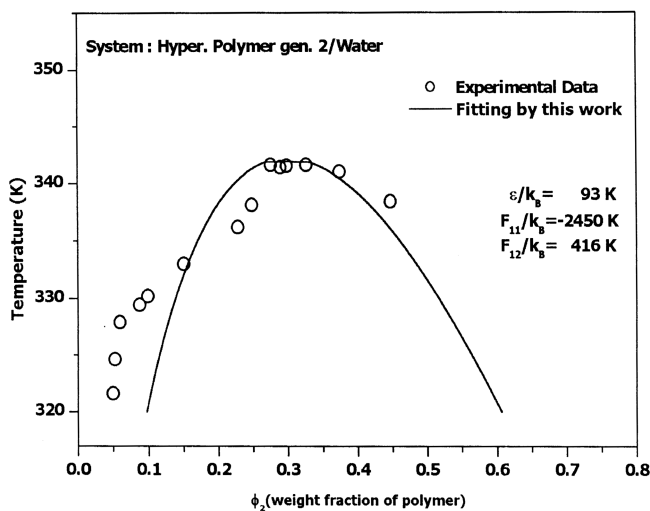


Fig. 3. Coexistence curve for the hyperbranched polymer generation 2/water system open circles are experimental data and the solid line is calculated by this work.

water systems. Structures of hyperbranched polymers are given in Table 3 and the simplified molecular structure of hyperbranched polymer generation 2 is given in Fig. 2a [Jang and Bae, 2001].

Because the presence of linear segments in molecules makes a difference between structures of hyperbranched polymer and dendrimer, it is difficult to determine the separator length of the hyperbranched polymer. We set n as a mean separator length of the given system.

In Fig. 3, we compare experimental cloud point data for hyperbranched polymer generation 2/water system with the calculated coexistence curve. Open circles indicate experimental data [Jang and Bae, 2001]. The solid line is calculated by this work. The separator length (n) and coordination number (z) are 4 and 8, respectively. We determined the model parameters on the basis of the critical point and the tie line for a given system. The procedures are given in the appendix. The parameter values are $\epsilon/k_B=93$ K, $F_{11}^H/k_B=-2,450$ K, and $F_{12}^H/k_B=416$ K. The calculated coexistence curve shows a slight deviation in the dilute polymer concentration region.

Fig. 4 represents comparison of experimental cloud point data for hyperbranched polymer generation 3/water with the model. Open circles are experimental data [Jang and Bae, 1999]. The solid line is calculated by this work. The parameter values are $\epsilon/k_B=90.3$ K (Kelvin), $F_{11}^H/k_B=-3,650$ K, and $F_{12}^H/k_B=50$ K. The model gives a fairly good agreement with experimental data.

Fig. 5 shows the coexistence curve for the hyperbranched polymer generation 4/water system. Open circles are experimental data [Jang and Bae, 1999] and the solid line is calculated by this work. The parameter values are $\epsilon/k_B=103$ K (Kelvin), $F_{11}^H/k_B=-3,750$ K, and

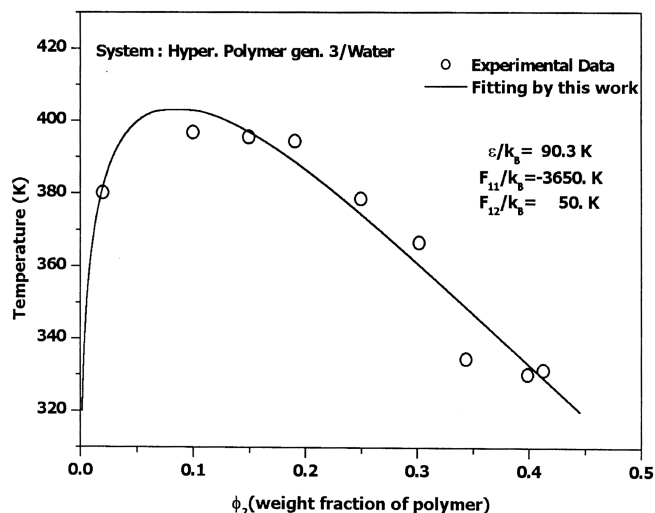


Fig. 4. Coexistence curve for the hyperbranched polymer generation 3/water system open circles are experimental data and the solid line is calculated by this work.

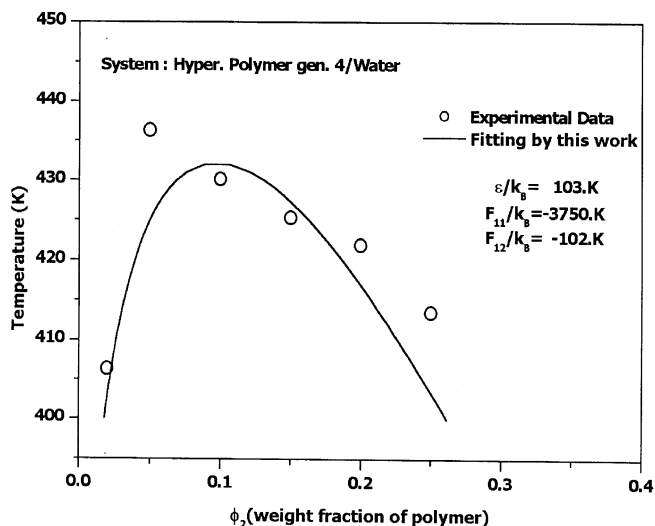


Fig. 5. Coexistence curve for the hyperbranched polymer generation 4/water system open circles are experimental data and the solid line is calculated by this work.

$F_{12}^H/k_B=-100$ K. There is a slight deviation between the calculated coexistence curve and experimental data. All the given systems show that the specific interaction energy between solvent molecules is much higher than that between the solvent and the endgroups. This is because the lower value of hydrogen bonding gives more association. The hydrogen bonding between solvent molecules can be regarded as dominating the phase behavior of those systems. As the number of endgroups increases exponentially with the generation number, the effect of the hydrogen bonding between the solvent and the endgroup is growing. It is thought that the increase of solvent-endgroup hydrogen bonding energy provides another source of solvent-polymer interactions.

Secondly, we compared the proposed model with VLE experimental data of dendrimer solutions. Fig. 6 shows an activity of methanol at 35 °C in polyamidoamine (PAMAM) dendrimer ($g=1$). Open

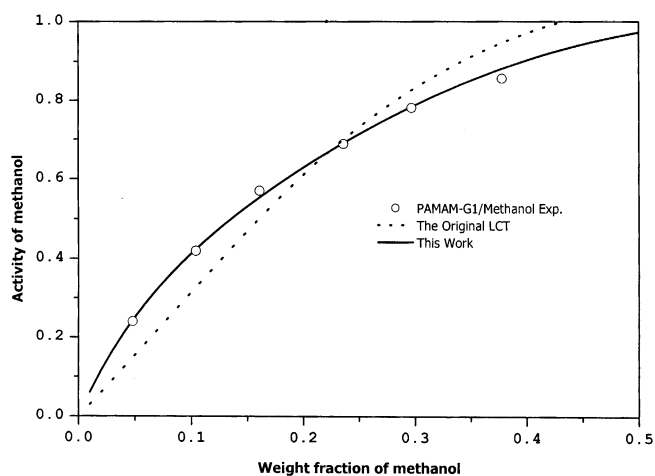


Fig. 6. Fits with LCT (the dotted line) and this work (the solid line) of VLE data for PAMAM-G1 in methanol at 35 °C (Open circles).

circles are VLE data by Mio et al. [1998]. The vapor pressure of the pure methanol is 27.9 kPa at 35 °C. The dotted line is calculated from the original LCT. We fixed the geometric parameters, separator length (n) and the number of core segments (n_0) as 3 and 3, respectively. It shows a slight deviation from experimental data. The interaction parameter ε/k_B is 93.53 K. The solid line is calculated from the proposed model with the same geometric parameters. Energy parameters are $\varepsilon/k_B=66.58$ K, $F_{11}^S/k_B=2,634.56$ K and $F_{12}^S/k_B=-733.38$ K. From the relation of Eqs. (23) and (24), the number of specific interactions increases with decreasing interaction energy. The fraction of solvent-solvent interaction, v_{11} , varies from 0.003 to 1.002×10^{-7} and v_{12} changes from 0.0944 to 0.001. It means that the interaction energy between methanol and endgroups of PAMAM is much greater than that between solvents in this system.

Fig. 7 shows an activity of methanol at 35 °C in (PAMAM) dendrimer ($g=2$). Open circles are VLE data by Mio [Mio et al., 1998]. The dotted line is calculated from the original LCT and the solid line is from this work with the same geometric parameters except for

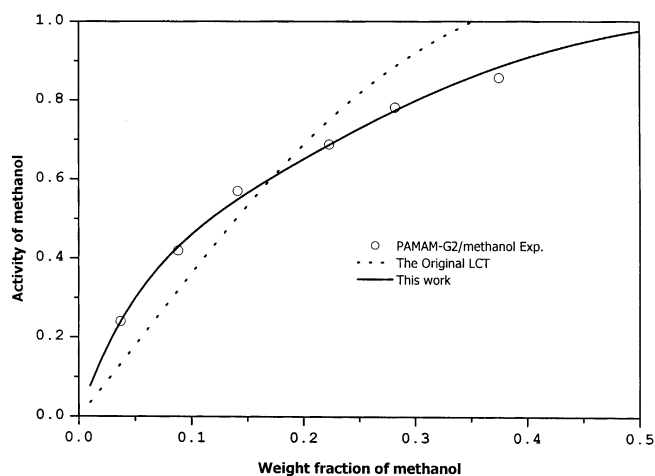


Fig. 7. Fits with LCT (the dotted line) and this work (the solid line) of VLE data for PAMAM-G2 in methanol at 35 °C (Open circles).

generation number. Energy parameter from LCT is $\varepsilon/k_B=101.90$ K. For the proposed model, $\varepsilon/k_B=67.01$ K, $F_{11}^S/k_B=2,352.14$ K and $F_{12}^S/k_B=-783.05$ K. The solvent-endgroup interaction dominates the chemical contribution in this system similar to that of PAMAM-G1/methanol system. Those systems show consistency with the fact that PAMAM dendrimers are strongly hydrophilic polymer completely miscible in the lower alcohol. Compared with the LCT model, the proposed model taking into account the specific interaction contribution term gives better agreement with experimental data. In these systems, the solvent-solvent interactions are negligible.

Finally, we choose benzyl ether dendrimer/toluene system as a model system for simulation approach. The model structure of dendrimer is given in Fig. 8(a). The types of monomer units are divided into two parts: innergroups and endgroups. Figs. 8(b)-(d) represent structures of innergroup, endgroup 1 and endgroup 2, respectively. The structures of innergroup, endgroup 1, endgroup 2 and toluene are optimized with the DREIDING II force field. The relative sizes of polymer segments (innergroup and endgroup 1) and the solvent molecule are almost identical. The molecular surface area and volume are calculated by using the van der Waals radii of the atoms in the molecule. Such a definition of lattice size, however, is regarded with caution, as it may not be generally applicable.

In Fig. 8(b)-(d), "c"s indicate the dummy atoms. Because the polymer segment is connected with the other segments, we consider

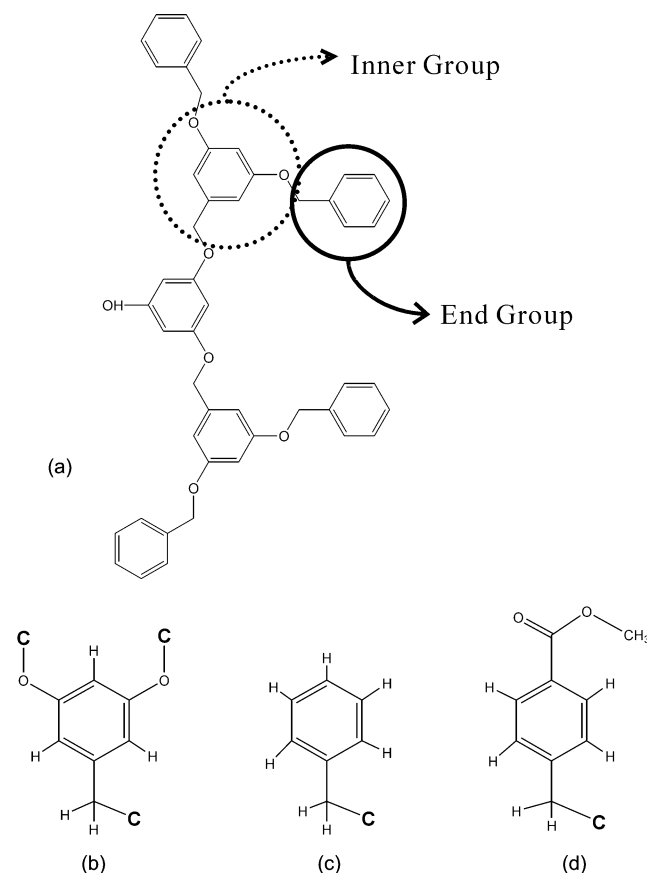


Fig. 8. The model structure of dendrimer (a) and types of monomer units (b-d). (b), (c) and (d) represent structures of innergroup, endgroup 1 and endgroup 2, respectively. "c"s indicate the dummy atoms.

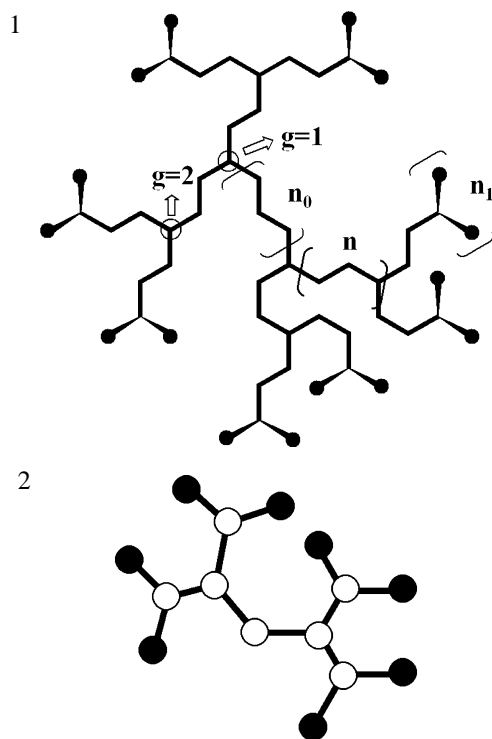


Fig. 9. 1, Simplified general structure of dendrimer generation 2. Dark circles represent endgroups. g , n_0 , and n mean the generation number, the number of segments in core, and the number of segments between generation points. 2, Simplified benzyl ether dendrimer structure. Dark circles and open circles represent endgroups and innergroups, respectively.

the effect of chain connectivity by introducing dummy atoms at the connecting positions of the polymer segments, making some position of polymer segments inaccessible to the other segments. The dummy atoms are considered a methyl group in the united atom approximation. In the calculation of the number of configurations, any configuration containing contacts with dummy atoms is rejected and the interaction energies associated with the dummy atoms are not calculated. For each calculation 30,000 of the molecular pairs are generated.

Structures of dendrimers examined in this study are given in Fig. 8. We simplify these general structures as two types as shown in Fig. 9-1. Dark circles represent endgroups. Given dendrimers, in this study, are characterized by three parameters: the generation number, the number of segments in core, and the number of segments between generation points. In Fig. 9-2, we give a simplified structure for benzyl ether dendrimer. Because this structure is connected with only a generation point, we give indices for this structure in Table 1. Pair interaction energies determined from simulations are listed in previous work [Jang and Bae, 2002]. We choose the arithmetic mean of ϵ_{12} and ϵ_{21} for the single solvent-polymer interaction energy parameter (ϵ_{12}) in physical contribution to Helmholtz free energy. From the simulation results attractions for pairs are given as negative pair potential. Because the interaction energy is defined as the energy required to separate two bodies to infinite intermolecular separation, we take the absolute value of potential as the interaction energy. We define the specific interaction energy for end-

groups (F_{22}^s) as the difference between the endgroup-endgroup interaction energy and the innergroup-innergroup interaction energy. Also, the specific interaction energy for endgroup and solvent (F_{12}^s) is defined as the difference between the endgroup-toluene interaction energy and the innergroup-solvent interaction energy.

We assume that a solvent molecule has one specific interaction donor site. The dendrimer molecules have both donor and acceptor sites. The number of donor sites of solvent (d_1) is a unity and the numbers of acceptor sites and donor sites (a_2 and d_2) are the same as the number of end groups of polymer molecules. Thus, there are two types of specific interactions in the given systems. Helmholtz free energy and chemical potential of solvent are

$$\beta A^s = M_{12} + M_{22} + N_1 d_1 \ln \left(1 - \frac{M_{12}}{N_1 d_1} \right) + N_2 d_2 \ln \left(1 - \frac{M_{22}}{N_2 d_2} \right) + N_2 a_2 \ln \left(1 - \frac{M_{12} + M_{22}}{N_2 a_2} \right) \quad (28)$$

$$\beta \frac{\partial A^s}{\partial N_1} = \beta \mu_1^s = d_1 \ln \left(1 - \frac{v_{12}}{\phi_1 d_1} \right) + \frac{d_1 v_{12}}{\phi_1 d_1 - v_{12}} \quad (29)$$

where $v_{12} = M_{12}/N$, and $v_{22} = M_{22}/N$

Minimizing Eq. (10), gives

$$N M_{12} = (N_1 d_1 - M_{11})(N_2 a_2 - M_{12} - M_{22}) \exp \left(-\frac{F_{12}^s}{k_B T} \right) \quad (30)$$

$$N M_{22} = (N_2 d_2 - M_{22})(N_2 a_2 - M_{12} - M_{22}) \exp \left(-\frac{F_{22}^s}{k_B T} \right) \quad (31)$$

From Eqs. (29)-(31), we obtain the activity of solvent molecule for a given system. We calculate the numbers of specific interactions by solving Eqs. (30) and (31) simultaneously. Fig. 10 shows an activity of toluene at 70 °C in polybenzyl ether dendrimer with endgroup 1 (generation 4). Open circles are VLE data by Mio et al. [1998]. The vapor pressure of the pure toluene is 30.1 kPa at 70 °C. The solid line is calculated from this work. In this study, we do not fit experimental data to the model to determine adjustable parameters. Those parameters are calculated by molecular simulation. The dotted line is calculated from the original LCT. Separator length

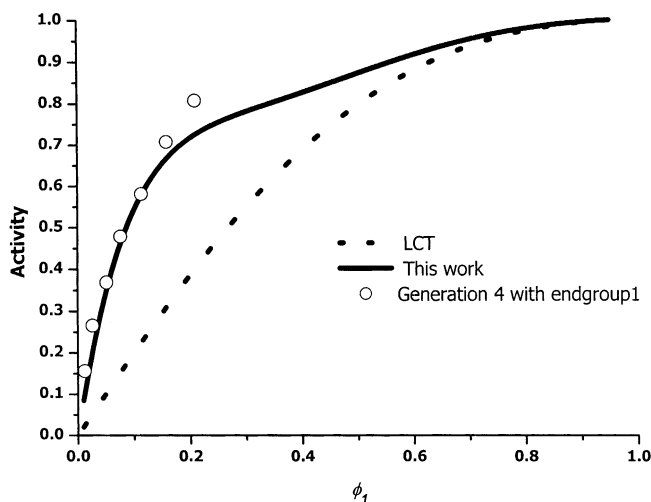


Fig. 10. Prediction with LCT (the dotted line) and this work (the solid line) of VLE data for benzyl ether dendrimer generation 4 with endgroup 1 in toluene at 70 °C (Open circles).

(n) and the number of core segments (n_0) are 1 and 1, respectively. From the simulation results, $\varepsilon/k_B=1.47$ K, $F_{22}^s/k_B=-572.35$ K and $F_{12}^s/k_B=-257.75$ K. F_{22}^s is calculated by the difference between endgroup 1-endgroup 1 interaction energy (ε_{22}) and innergroup-innergroup interaction energy and F_{12}^s is considered as the difference between endgroup 1-solvent interaction energy (ε_{12}) and innergroup-solvent interaction energy. As shown in Fig. 10, the specific interaction consideration associated with endgroups correlates with the experimental data.

Fig. 11 presents fractions of specific interactions with dendrimer concentration for the same system in Fig. 4. The fraction of (i, j) pair specific interaction (v_{ij}) is the ratio between the number of the (i, j) pair interaction and the number of total lattice sites ($v_{ij}=M_{ij}/N$). The specific interaction of endgroup-solvent pair (v_{12}) is greater than that of endgroup-endgroup pair (v_{22}). This explains that the endgroup-solvent specific interaction is a major factor in VLE of

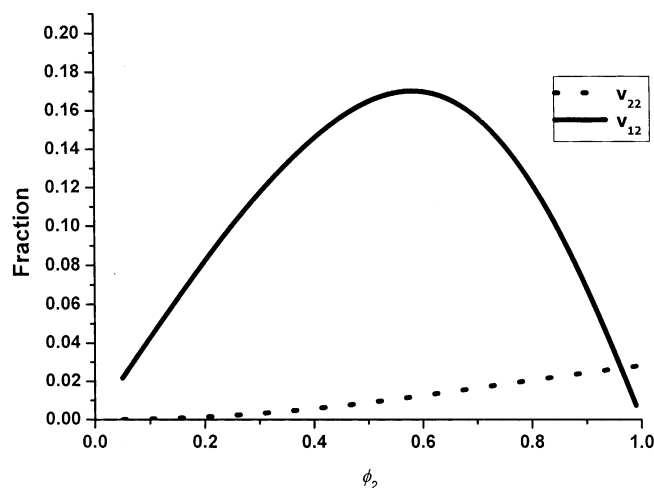


Fig. 11. Fractions of specific interactions with polymer concentration. v_{12} and v_{22} are specific interactions of endgroup-solvent pair and endgroup-endgroup in the system given in Fig. 4, respectively.

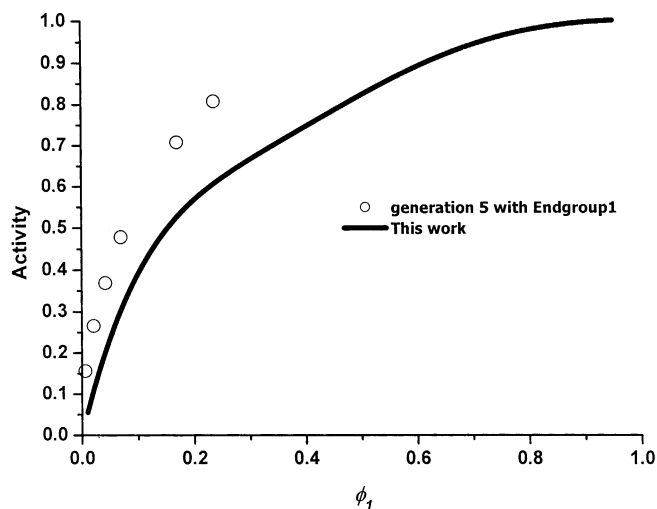


Fig. 12. Comparison with VLE data for benzyl ether dendrimer generation 5 with endgroup 1 in toluene at 70 °C (Open circles).

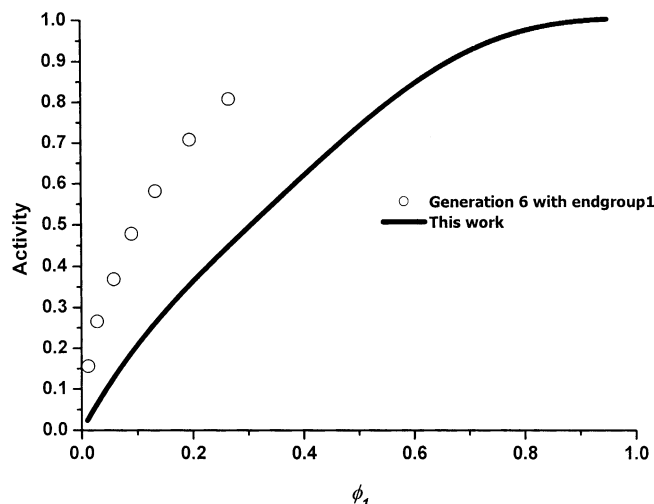


Fig. 13. Comparison with VLE data for benzyl ether dendrimer generation 6 with endgroup 1 in toluene at 70 °C (Open circles).

dendrimer solution. In this calculation, we set the coordination number z as 12 for the entire calculation.

Figs. 12 and 13 exhibit an activity of toluene at 70 °C in benzyl ether dendrimer generations 5 and 6 with endgroup 1, respectively. Open circles are VLE data obtained by Mio et al. [1998]. The solid line is calculated with the same geometric parameters and interaction energies except the generation number as shown in Fig. 10. The deviation from the experimental data increases with the generation number. It may be due to the increase of steric hindrance from crowded endgroups at periphery of dendrimer molecule with the increase of the generation number. In VLE of benzyl ether dendrimer/toluene system with higher generations, the solvent-endgroup interaction also dominates the additional contribution in this system.

An activity data of toluene at 70 °C in benzyl ether dendrimer generation 4 with endgroup 2 and hypothetical predictions for higher generation are presented in Fig. 8. Open circles are experimental data [Mio et al., 1998]. The solid line is calculated with the same geometric parameters as in the case of dendrimer with endgroup 1. Because of the lack of experimental data, we give only theoretical predictions for generation 5 (dashed) and 6 (dotted). The energy parameters for benzyl ether dendrimer with endgroup 2 are $\varepsilon/k_B=1.47$ K, $F_{22}^s/k_B=280.673$ K and $F_{12}^s/k_B=32.563$ K. We define specific interactions (F_{22}^s and F_{12}^s) as differences of interaction energies with respect to innergroup as a reference segment. Therefore, ε/k_B is the same as in the case of endgroup 1. The difference of specific interaction between endgroup 1 and endgroup 2 is due to their different structures. Endgroup 2 has acetate functional group at para position. The specific interaction energy of endgroup 2 is higher than that of endgroup 1. It shows that intermolecular forces of endgroup 2 are more attractive than those of endgroup 1. Simulation results go well with experimental phenomena. From experimental data in Figs. 10 and 14, the activity of dendrimer with endgroup 2 is slightly higher than that of dendrimer with endgroup 1. However, a reverse case occurs with the increase of solvent. As shown in Fig. 11, the number of (2, 2) pairs (M_{22}) decreases but the number of (1, 2) pairs (M_{12})

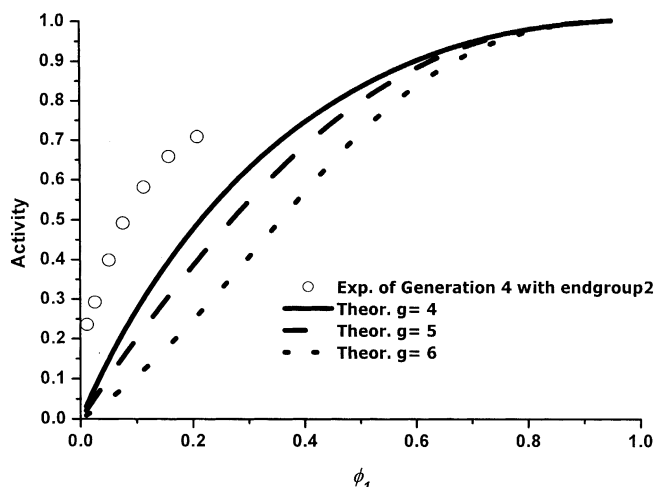


Fig. 14. Comparison with VLE data for benzyl ether dendrimer generation 4 with endgroup 2 in toluene at 70 °C (Open circles).

increases drastically. Because the cross association (12 pairs) is unfavorable to activity of solvent, the activity of dendrimer with endgroup 2 comes to be lower than that of dendrimer with endgroup 1.

In optimizing structures, interatomic interaction energies calculated from this work show a great dependence on the force field applied. Hence, it is essential to apply a proper force field for given structures in predicting phase equilibria of polymer systems. In addition, the size difference between segments of each component and the single type of coordination number z still remain difficulties in bridging theories based on statistical thermodynamics with the molecular simulation technique.

CONCLUSION

We have developed and examined the thermodynamic framework to describe phase behavior of dendritic polymers systems with highly branched structure and specific interactions. In liquid-liquid equilibria of hyperbranched polymer aqueous solution, the specific interaction energy between solvent molecules is much higher than that between the solvent and the end-group for all given systems. Our results show that the solvent-solvent specific interaction dominates the phase behavior of hyperbranched polymer/water systems. However, the end groups of hyperbranched polymers also play a great role in determining phase separation of a polymer system with highly branched structure. It means that the type of end-group is one of the major factors in non-aqueous polar solvent system. All the results given in this work are for homogeneous and monodisperse hyperbranched polymer, i.e. polymer with identical segments except for end-groups. However, hyperbranched polymers used in many interesting applications are neither homogeneous nor monodisperse. In a typical hyperbranched polymer, segments inside are different from those at the periphery and there is a distribution of separator length.

In comparison with VLE data, this work shows that the specific interaction between solvent molecules is much smaller than that between the solvent and the end-group for PAMAMs in methanol and benzyl dodecyl dendrimers in toluene. Our results show that

the solvent-endgroup specific interaction dominates VLE of dendrimer in solvent. It means that the type of end-group is one of the major factors determining VLE in dendrimer/solvent systems. Because the LCT used here is truncated after a finite number of terms, it only accounts for a short-range correlation between polymer segments. Therefore, predictions from the LCT should be regarded with caution, especially for higher-generation dendrimers.

For the prediction of the activity for systems of dendrimers, structured polymers with numerous branches and effective endgroup in the application of molecular simulation approach, we considered the specific interactions among endgroups and solvents and used the pairs method including Monte Carlo sampling method and excluded volume constraint in molecular simulation. Calculated results for VLE of dendrimer solutions show some deviation from experimental data in higher generation system. In this study, we obtained all parameters by using molecular simulation. We did not fit the experimental data to the model to determine model parameters. However, the difference between the segmental size and the definition of lattice size in lattice model, the rationalization of the coordination number z and the dependence on the force field need to be improved to correlate the phase behavior of polymer systems. Nevertheless, this approach shows that the combination of molecular simulation and the statistical modeling can be the substitute of fully atomistic molecular mechanics or molecular dynamics, which face the difficulties of time and space scale in polymer thermodynamics.

ACKNOWLEDGMENT

This work was conducted with the support of Korea Institute of Science & Technology Evaluation and Planning (KISTEP) under National Research Laboratory (NRL) Program.

APPENDIX

Critical Point conditions are given as

$$\frac{\partial \mu}{\partial \phi_2} = \frac{\partial \mu_2^{LCT}}{\partial \phi_2} + \frac{\partial \mu_2^H}{\partial \phi_2} = 0 \quad (\text{A-1})$$

$$\frac{\partial^2 \mu}{\partial \phi_2^2} = \frac{\partial^2 \mu_2^{LCT}}{\partial \phi_2^2} + \frac{\partial^2 \mu_2^H}{\partial \phi_2^2} = 0 \quad (\text{A-2})$$

where

$$\begin{aligned} \frac{\partial}{\partial \phi_2} \beta \mu_2^{LCT} = & \frac{1}{M \phi_2} + \left(1 - \frac{1}{M}\right) \\ & + a^{(0)} 2(-1 + \phi_2) + a^{(1)} 2(-1 + \phi_2)(-1 + 3\phi_2) + a^{(2)} 6(-1 + \phi_2)\phi_2(-1 + 2\phi_2) \\ & + A^{(1)} 2(-1 + \phi_2) - 2(A^{(2)} + B^{(3)})(-1 + \phi_2)(1 - 6\phi_2 + 6\phi_2^2) \\ & - 2A^{(3)}(-1 + \phi_2)(1 - 18\phi_2 + 78\phi_2^2 - 120\phi_2^3 + 60\phi_2^4) \\ & - 2A^{(4)}(-1 + \phi_2)(1 - 42\phi_2 + 330\phi_2^2 - 1080\phi_2^3 + 1800\phi_2^4 - 1512\phi_2^5 + 504\phi_2^6) \\ & - 2(B^{(1)} + B^{(2)})(-1 + \phi_2)(-2 + 3\phi_2) - 2B^{(4)}(-1 + \phi_2)\phi_2(3 - 12\phi_2 + 10\phi_2^2) \\ & - 2C^{(1)}(-1 + \phi_2)(-6 + 39\phi_2 - 72\phi_2^2 + 40\phi_2^3) + C^{(2)} 6(-1 + \phi_2)^2(-1 + 2\phi_2) \\ & - 2C^{(3)}(1 - \phi_2)^2(-1 + 17\phi_2 - 55\phi_2^2 + 45\phi_2^3) - 4C^{(4)}(-1 + \phi_2)^3(-2 + 5\phi_2) \quad (\text{A-3}) \end{aligned}$$

$$\frac{\partial}{\partial \phi_2} \beta \mu_2^H = \frac{a_2 M^2 v_{12} \left(\phi_2 \frac{\partial v_{12}}{\partial \phi_2} - v_{12} \right)}{\phi_2 (a_2 \phi_2 - M v_{12})^2} \quad (\text{A-4})$$

The first derivative of v_{12} with respect to ϕ_2 is calculated by differentiating Eqs. (33) and (34) with respect to ϕ_2 . It is calculated directly

by the following two elements simultaneous equation

$$(2v_{11} + v_{12} - a_1\phi_1 - d_1\phi_1 - 1/A_{11})\frac{\partial v_{11}}{\partial \phi_2} + (v_{11} - a_1\phi_1)\frac{\partial v_{12}}{\partial \phi_2} = d_1(a_1\phi_1 - v_{11}) + a_1(d_1\phi_1 - v_{11} - v_{12}) \quad (\text{A-5})$$

$$\left(v_{12} - \frac{a_2\phi_2}{M}\right)\frac{\partial v_{11}}{\partial \phi_2} + \left(v_{11} + 2v_{12} - d_1\phi_1 - \frac{a_2\phi_2}{M} - \frac{1}{A_{12}}\right)\frac{\partial v_{12}}{\partial \phi_2} = d_1\left(\frac{a_2\phi_2}{M} - v_{12}\right) - \frac{a_2}{M}(d_1\phi_1 - v_{11} - v_{12}) \quad (\text{A-6})$$

$$\begin{aligned} \frac{\partial^2}{\partial \phi_2^2} \beta \mu_2^{LCR} = & -\frac{1}{M\phi_2^2} + 2a^{(0)} + 4a^{(1)}(-2 + 3\phi_2) + a^{(2)}6(1 - 6\phi_2 + 6\phi_2^2) \\ & + 2A^{(1)} - 2(A^{(2)} + B^{(3)})(7 - 24\phi_2 + 18\phi_2^2) \\ & - 2A^{(3)}(19 - 192\phi_2 + 594\phi_2^2 - 720\phi_2^3 + 300\phi_2^4) \\ & - 2A^{(4)}(43 - 744\phi_2 + 4230\phi_2^2 - 11520\phi_2^3 + 16560\phi_2^4 - 12096\phi_2^5 + 3528\phi_2^6) \\ & - 2(B^{(1)} + B^{(2)})(-5 + 6\phi_2) - 2B^{(4)}(-3 + 30\phi_2 - 66\phi_2^2 + 40\phi_2^3) \\ & - 2C^{(1)}(-3 + 4\phi_2)(15 - 54\phi_2 + 40\phi_2^2) + 12C^{(2)}(-1 + \phi_2)(-2 + 3\phi_2) \\ & - 2C^{(3)}(-1 + \phi_2)(-19 + 161\phi_2 - 355\phi_2^2 + 225\phi_2^3) \\ & - 4C^{(4)}(-1 + \phi_2)^2(-11 + 20\phi_2) \end{aligned} \quad (\text{A-7})$$

$$\begin{aligned} \frac{\partial^2 \beta \mu_2^H}{\partial \phi_2^2} = & \frac{a_2 M^2 \left[\left(\frac{\partial v_{12}}{\partial \phi_2} \right)^2 \phi_2 + v_{12} \frac{\partial v_{12}}{\partial \phi_2} + \phi_2 v_{12} \frac{\partial^2 v_{12}}{\partial \phi_2^2} - 2v_{12} \frac{\partial v_{12}}{\partial \phi_2} \right]}{\phi_2 (a_2 \phi_2 - Mv_{12})^2} \\ & - \frac{(a_2 \phi_2 - Mv_{12}) \left(a_2 \phi_2 - Mv_{12} + 2a_2 \phi_2 - 2\phi_2 M \frac{\partial v_{12}}{\partial \phi_2} \right) a_2 M^2 v_{12} \left(\phi_2 \frac{\partial v_{12}}{\partial \phi_2} - v_{22} \right)}{\phi_2^2 (a_2 \phi_2 - Mv_{12})^4} \end{aligned} \quad (\text{A-8})$$

The second derivative of v_{12} with respect to ϕ_2 is calculated by differentiating Eqs. (A-5) and (A-6) with respect to ϕ_2 . It is also calculated directly by the following two elements simultaneous equation:

$$(2v_{11} + v_{12} - a_1\phi_1 - d_1\phi_1 - 1/A_{11})\frac{\partial^2 v_{11}}{\partial \phi_2^2} + (v_{11} - a_1\phi_1)\frac{\partial^2 v_{12}}{\partial \phi_2^2} = d_1\left(-a_1 - \frac{\partial v_{11}}{\partial \phi_2}\right) + a_1\left(-d_1 - \frac{\partial v_{11}}{\partial \phi_2} - \frac{\partial v_{12}}{\partial \phi_2}\right) - \left(a_1 + \frac{\partial v_{11}}{\partial \phi_2}\right)\frac{\partial v_{12}}{\partial \phi_2} - \frac{\partial v_{11}}{\partial \phi_2}\left(a_1 + d_1 + 2\frac{\partial v_{11}}{\partial \phi_2} + \frac{\partial v_{12}}{\partial \phi_2}\right) \quad (\text{A-9})$$

$$\begin{aligned} \left(v_{12} - \frac{a_2\phi_2}{M}\right)\frac{\partial^2 v_{11}}{\partial \phi_2^2} + \left(v_{11} + 2v_{12} - d_1\phi_1 - \frac{a_2\phi_2}{M} - \frac{1}{A_{12}}\right)\frac{\partial^2 v_{12}}{\partial \phi_2^2} = & d_1\left(\frac{a_2}{M} - \frac{\partial v_{12}}{\partial \phi_2}\right) - \frac{a_2}{M}(-d_1 - v_{11} - v_{12}) \\ & + \frac{\partial v_{11}}{\partial \phi_2}\left(\frac{a_2}{M} - \frac{\partial v_{12}}{\partial \phi_2}\right) - \frac{\partial v_{12}}{\partial \phi_2}\left(d_1 - \frac{a_1}{M} + \frac{\partial v_{11}}{\partial \phi_2} + 2\frac{\partial v_{12}}{\partial \phi_2}\right) \end{aligned} \quad (\text{A-10})$$

The tie line conditions are

$$\Delta \mu_1' = \Delta \mu_1'' \quad (\text{A-11})$$

$$\Delta \mu_2' = \Delta \mu_2'' \quad (\text{A-12})$$

REFERENCES

- Allen, M. P. and Tildesley, D. J., "Computer Simulation of Liquids," Clarendon Press, Oxford, England (1987).
 Aranovich, G. L. and Donhue, M. D., "A New Model for Lattice Systems," *J. Chem. Phys.*, **105**, 7059 (1996).
 Backer, J. A. and Fock, W., *Discuss. Faraday Soc.*, **15**, 188 (1953).

- Baschnagel, J., Binder, K., Paul, W., Laso, M., Suter, U. W., Batoulis, I., Jilge, W. and Bürger, T., "On the Construction of Coarse-grained Models for Linear Flexible Polymer Chains: Distribution Functions for Groups of Consecutive Monomers," *J. Chem. Phys.*, **95**, 601 (1991).
 Bawendi, M. G., Freed, K. F. and Mohanthy, U., "A Lattice Field Theory for Polymer Systems with Nearest-neighbor Interaction Energies," *J. Chem. Phys.*, **87**, 5534 (1988a).
 Bawendi, M. G., Freed, K. F. and Mohanthy, U., "Systematic Corrections to Flory-Huggins Theory: Polymer-solvent-void Systems and Binary Blend-void Systems," *J. Chem. Phys.*, **88**, 2741 (1988b).
 Binder, K. and Heermann, D. W., "Monte Carlo Simulation in Statistical Physics," Springer-Verlag, Berlin (1988).
 Blanco, M., "Molecular Silverware. I. General Solutions to Excluded Volume Constrained Problems," *J. Comput. Chem.*, **12**, 237 (1991).
 Burtkert, U. and Allinger, N. L., "Molecular Mechanics," American Chemical Society, Washington, DC (1982).
 Chang, J. and Kim, H., "Molecular Dynamic Simulation and Equation of State of Lennard-Jones Chain Fluids," *Korean J. Chem. Eng.*, **15**, 544 (1998).
 Dagani, R., "Chemist Explore Potential of Dendritic Macromolecules as Functional Materials," *C&EN*, June 3, 30 (1996).
 Dudowicz, J. and Freed, K. F., "Effect of Monomer Structure and Compressibility on the Properties of Multicomponent Polymer Blends and Solutions: 1. Lattice Cluster Theory of Compressible Systems," *Macromolecules*, **24**, 5076 (1991).
 Dudowicz, J., Freed, M. S. and Freed, K. F., "Effect of Monomer Structure and Compressibility on the Properties of Multicomponent Polymer Blends and Solutions: 1. Lattice Cluster Theory of Compressible Systems," *Macromolecules*, **24**, 5096 (1991).
 Fan, C. F., Olafson, B. D., Blanco, M. and Hsu, S. L., "Application of Molecular Simulation to Derive Phase Diagrams of Binary Mixtures," *Macromolecules*, **25**, 3667 (1992).
 Flory, P. J., "Principles of Polymer Chemistry," Cornell University, Ithaca (1953).
 Freed, K. F. and Bawendi, M. G., "Lattice Theories of Polymeric Fluids," *J. Phys. Chem.*, **93**, 2194 (1989).
 Freed, K. F. and Dudowicz, J., "Role of Monomer Structure and Compressibility on the Properties of Multicomponent Polymer Blends and Solutions. 4. High Molecular-Weights, Temperature Dependences, and Phase-Diagrams of Binary Polymer Blends," *J. Theor. Chim. Acta*, **82**, 357 (1992).
 Freed, K. F., "New Lattice Model for Interacting, Avoiding Polymers with Controlled Length Distribution," *J. Phys. A; Math. Gen.*, **18**, 871 (1985).
 Fréchet, J. M. J., "Functional Polymers and Dendrimers - Reactivity, Molecular Architecture, and Interfacial Energy," *Science*, **263**, 1710 (1994).
 Guggenheim, E. A., "Mixtures," Clarendon Press, Oxford (1952).
 Hawker, C. J., Farington, P. J., McKay, M. E., Wooley, K. L. and Fréchet, J. M. J., "Molecular Ball-Bearings - The Unusual Melt Viscosity Behavior of Dendritic Macromolecules," *J. Am. Chem. Soc.*, **117**, 4409 (1995).
 Huggins, M. L., "Solutions of Long Chain Compounds," *J. Chem. Phys.*, **9**, 440 (1941).
 Jang, J. G. and Bae, Y. C., "Phase Behavior of Hyperbranched Polymer Solutions with Specific Interactions," *J. Chem. Phys.*, **114**, 503 (2001).

- Jang, J. G. and Bae, Y. C., "Phase Behaviors of Dendrimer/Solvent Systems: Molecular Thermodynamics Approach," *J. Chem. Phys.*, **116**, 3484 (2002).
- Jang, J. G. and Bae, Y. C., "Phase Behaviors of Hyperbranched Polymer Solutions," *Polymer*, **40**, 676 (1999).
- Jo, W. H. and Choi, K., "Determination of Equation-of-State Parameters by Molecular Simulations and Application to the Prediction of Surface Properties for Polyethylene," *Macromolecules*, **30**, 1800 (1997).
- Johansson, M., Malmström, E. and Hult, A., "The Synthesis and Properties of Hyperbranched Polyesters," *Trends. Poly. Sci.*, **4**, 398 (1996).
- Jung, J. K., Joung, S. N., Shin, H. Y., Kim, S. Y., Yoo, K., Huh, W. and Lee, C. S., "Measurements and Correlation of Hydrogen-Bonding Vapor Sorption Equilibrium Data of Binary Polymer Solutions," *Korean J. Chem. Eng.*, **19**, 296 (2002).
- Kim, S., Song, J., Chang, J. and Kim, H., "Prediction of Nonrandom Mixing in Lattice Model with Multi-references," *Korean J. Chem. Eng.*, **18**, 159 (2001).
- Kim, Y. H., Nelso, J. T. and Glynn, A. B., "Meso-scale Modeling of Polymers and its Applications in Food Technology," *Cereal Foods World*, **39**, 8 (1994).
- Mio, C., Kiritsov, S., Thio, Y., Brafman, R. and Prausnitz, J. M., "Vapor-Liquid-Equilibria for Solutions of Dendritic Polymers," *J. Chem. Eng. Data*, **43**, 541 (1998).
- Monnerie, L. and Suter, U. W., Eds., "Advances in Polymer Science," Springer-Verlag, Berlin, **116** (1994).
- Nemirovsky, A. M., Bawendi, M. G. and Freed, K. F., "Lattice Models of Polymer Solutions: Monomers Occupying Several Lattice Sites," *J. Chem. Phys.*, **87**, 7272 (1987).
- Nemirovsky, A. M., Dudowicz, J. and Freed, K. F., "Dense Self-Interacting Lattice Trees with Specified Topologies - From Light to Dense Branching," *Phys. Rev. A*, **45**, 7111 (1992).
- Panayiotou, C. G. and Sanchez, I. C., "Hydrogen Bonding in Fluids: An Equation-of-State Approach," *J. Phys. Chem.*, **95**, 10090 (1991).
- Panayiotou, C. G. and Vera, J. H., "The Quasi-chemical Approach for Non-randomness in Liquid Mixtures. Expressions for Local Surfaces and Local Compositions with an Application to Polymer Solutions," *Fluid Phase Equilib.*, **5**, 55 (1980).
- Panayiotou, C. G., "Lattice-fluid Theory of Polymer Solutions," *Macromolecules*, **20**, 861 (1987).
- Renuncio, J. A. R. and Prausnitz, J. M., "An Approximation for Non-randomness in Polymer-solution Thermodynamics," *Macromolecules*, **9**, 898 (1976).
- Roe, R. J., Ed., "Computer Simulation of Polymers," Prentice Hall, Englewood Cliffs, NJ (1991).
- Sanchez, I. C. and Balazs, A. C., "Generalization of the Lattice-fluid Model for Specific Interactions," *Macromolecules*, **22**, 2325 (1989).
- Schweizer, K. S. and Curro, J. G., "Integral Equation Theory of the Structure and Thermodynamics of Polymer Blends," *J. Chem. Phys.*, **91**, 5059 (1989).
- ten Brinke, G. and Karasz, F. E., "Lower Critical Solution Temperature Behavior in Polymer Blends: Compressibility and Directional-specific Interactions," *Macromolecules*, **17**, 815 (1984).
- Veystman, B. A., "Are Lattices Valid for Fluids with Hydrogen Bonds?," *J. Phys. Chem.*, **94**, 8499 (1990).